Measurement of the $D^0 \to \pi^- e^+ \nu$ Branching Fraction, Form Factor and Implications for $V_{\rm ub}$

Konrad Griessinger[1;1)] (for the *BABAR* Collaboration)

[1] Institute for Nuclear Physics, Mainz University, Germany

Abstract: The decay $D^0 \to \pi^- e^+ \nu$ is studied at the *BABAR* experiment using a sample of 500 million $c\bar{c}$ events recorded near the CM energy 10.6 GeV. Using this data, the branching fraction of the process $D^0 \to \pi^- e^+ \nu$ is extracted, as well as the hadronic form factor $f^{\pi}_{+,D}$ and the CKM matrix element $V_{\rm cd}$. Applying a relation between the decays $D^0 \to \pi^- e^+ \nu$ and $B^0 \to \pi^- e^+ \nu$, the matrix element $V_{\rm ub}$ is calculated and its precision will become competitive once new theoretical calculations appear.

Key words: BaBar, D^0, Branching Fraction, Form Factor, $V_{\rm cd}$, $V_{\rm ub}$

PACS: 13.25.Hw, 11.30.Er, 12.15.Hh

1 Introduction

The differential decay width of the process* $D^0 \to \pi^- e^+ \nu$ is parameterized by the CKM matrix element $V_{\rm cd}$ and – neglecting the electron mass – the form factor $f^{\pi}_{+,D}$, the only unknown function of q^2:

$$\frac{{\rm d}\Gamma}{{\rm d}q^2} = \frac{G_{\rm F}^2}{24\pi^3} \left(|V_{\rm cd}| \cdot \left|f^{\pi}_{+,D}(q^2)\right|\right)^2 p_{\pi}^{*3}(q^2) \ ,$$

where p_{π}^{*3} is the pion momentum in the D^0 rest frame. Therefore, by measuring the differential decay width, $V_{\rm cd}$ can be extracted by inserting a form factor from theory and conversely, the form factor can be extracted by assuming a value for $V_{\rm cd}$.

Furthermore, the decay $D^0 \to \pi^- e^+ \nu$ is related to the decay $B^0 \to \pi^- e^+ \nu$, such that $V_{\rm ub}$ can also be accessed.

2 Selection and Background Subtraction

The basic method of this analysis [1] is similar to previous studies [2] performed at *BABAR*. Two kinematic fits are performed: first, to the decay $D^{*+} \to D^0 \pi^+$, and subsequently to the final stage $D^0 \to \pi^- e^+ \nu$. This already gives a reasonably clean data sample, nonetheless further background suppression is necessary.

Since the decay $D^0 \to \pi^- e^+ \nu$ is Cabibbo-suppressed and there are large pionic backgrounds, a powerful background suppression is essential for this analysis. This is achieved using two different Fisher discriminants. The first discriminant $F_{b\bar{b}}$ is constructed to distinguish between the signal decay and $b\bar{b}$ events, which make up the majority of events at *BABAR*. The $b\bar{b}$ rest mass is not far below *BABAR*'s CM energy 10.58 GeV such that this type of event is produced almost at rest in the CM system. Thus the decay particles are distributed almost isotropically. Conversely, $c\bar{c}$ events including the signal decay possess a two-jet structure. This difference between the typical topologies can be exploited to distinguish the two classes. Therefore, the discriminant $F_{b\bar{b}}$ combines mostly event shape variables: R_2, the ratio between the second and zeroth order Fox-Wolfram moments [3, 4], the multiplicity of detected particles, and the momentum of the slow pion from the decay $D^{*+} \to D^0 \pi^+_s$. As shown in Fig. 1 (left), selecting only events with $F_{b\bar{b}} > 1.2$ results in good suppression of $b\bar{b}$ events.

The Fisher discriminant $F_{c\bar{c}}$ for rejecting $c\bar{c}$ events which are not the signal channel combines eight variables:

- D momentum,
- invariant mass of the spectators (particles not produced in c-quark fragmentation),
- direction of the total momentum of all spectators relative to the thrust axis,
- magnitude of the maximum spectator-momentum,
- direction of the spectator with the highest momentum relative to the thrust axis,
- direction of the spectator with the highest momentum relative to the D^0,
- direction of the lepton relative to the pion direction in the (e^+, ν_e) rest frame,
- charged lepton momentum in the CM frame.

Received 14 Nov. 2015

1) E-mail: griess@slac.stanford.edu

*Charge conjugation is implied throughout this paper.

Requiring $F_{c\bar{c}} > 0.6$ effectively rejects $c\bar{c}$-background as shown in Fig. 1 (right). After both Fisher selectors, a signal-to-noise ratio of ~ 1.2 and a signal efficiency of $\sim 1.8\,\%$ are achieved.

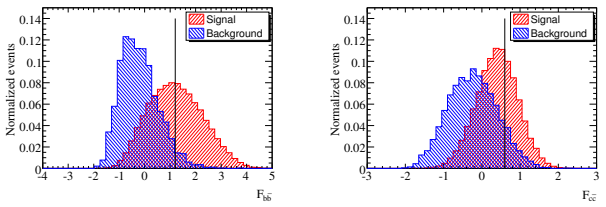

Fig. 1. Fisher discriminant distributions for $b\bar{b}$ and $c\bar{c}$ rejection in the signal and background simulation samples.

The background events remaining after the signal selection are treated using sideband subtraction. The signal and sideband regions are defined in the difference between the mass of the $D^0\pi$ system and the D^0 mass $\delta(m) = m(D^0\pi) - m_{D^0}$. The signal region is chosen as $\delta(m) < 0.155\,\text{GeV}$, while two sidebands are defined as $0.155\,\text{GeV} < \delta(m) < 0.2\,\text{GeV}$ and $0.2\,\text{GeV} < \delta(m) < 0.3\,\text{GeV}$. Both sidebands, shown in Fig. 2, are used to estimate the remaining background contributions using the event missing energy and the pion momentum. Therefore the main systematic uncertainty of this analysis is assessed using data. After adjusting the background contributions, it has been verified that there is good agreement between the well-known angular distribution in data and simulation.

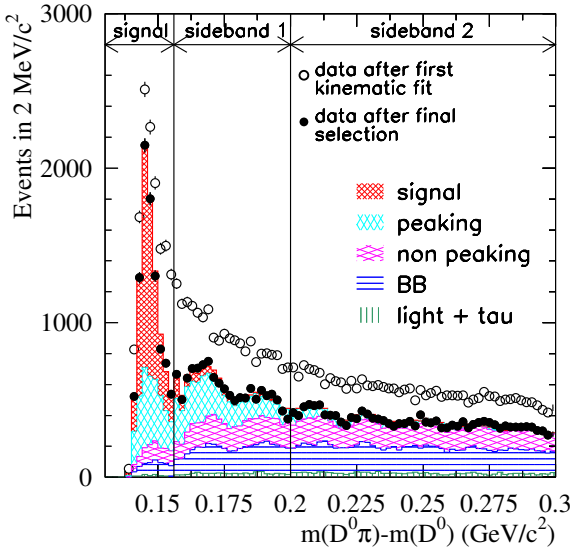

Fig. 2. Background subtraction using the sideband method.

Finally, the branching fraction is not measured as an absolute quantity but relative to the channel $D^0 \to K^-\pi^+$. Due to the similar selection criteria for both decays, many systematic uncertainties cancel out, improving the overall precision of the measurement.

3 Branching Fraction

Measuring the decay $D^0 \to \pi^- e^+ \nu$ relative to $D^0 \to K^-\pi^+$ leads to the branching ratio:

$$R_{\text{D}} = \frac{\mathcal{B}(D^0 \to \pi^- e^+ \nu)}{\mathcal{B}(D^0 \to K^-\pi^+)} = 0.0702 \pm 0.0017 \pm 0.0023\ ,$$

where the first uncertainty is statistical and the second systematic.

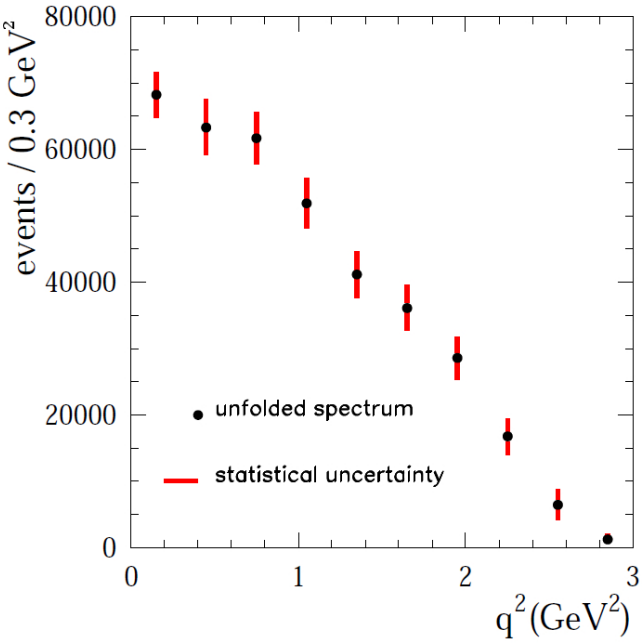

Fig. 3. Unfolded q^2 spectrum for $D^0 \to \pi^- e^+ \nu$ decays.

Using the Heavy Flavor Averaging Group's estimate [5] for $D^0 \to K^-\pi^+$ $\mathcal{B}(D^0 \to K^-\pi^+) = (3.946 \pm 0.052) \times 10^{-3}$, the following result for the absolute $D^0 \to \pi^- e^+ \nu$ branching fraction is obtained:

$$\mathcal{B}(D^0 \to \pi^- e^+ \nu) = (2.77 \pm 0.07 \pm 0.09 \pm 0.04) \times 10^{-3}\ ,$$

where the third uncertainty corresponds to the normalization channel. This value is compatible with the current world average [6] $\mathcal{B}(D^0 \to \pi^- e^+ \nu) = (2.89 \pm 0.08) \times 10^{-3}$.

4 Form Factor

After unfolding the event rate as a function of q^2 (where $q^2 = (p_{D^0} + p_{\pi^-})^2 = (p_{e^+} + p_\nu)^2$) from detector effects, the distribution shown in Fig. 3 is obtained. This distribution is used to probe several parameterizations of the form factor.

The first one to be investigated is called z-expansion. It has the great advantage of being model independent since it is only based on general properties of QCD [7]. The parameterization is expressed in terms of the variable

$$z(t,t_0) = \frac{\sqrt{t_+ - t} - \sqrt{t_+ - t_0}}{\sqrt{t_+ - t} + \sqrt{t_+ - t_0}} ,$$

with $t = q^2$, $t_0 = t_+(1 - \sqrt{1 - t_-/t_+})$, and $t_\pm = (m_{D^0} \pm m_{\pi^+})^2$. The form factor is now given as

$$f^\pi_{+,D}(t) = \frac{1}{\Phi(t,t_0)} \sum_{k=0}^{\infty} a_k(t_0) z^k(t,t_0) ,$$

where $\Phi(t,t_0)$ is an analytically known function [1]. The normalization is given by $V_{cd} f^\pi_{+,D}(0)$, such that the remaining fitting parameters can be expressed as $r_k = a_k/a_0$ $(k \geq 1)$, but possess no physical meaning. Using the *BABAR* data this results in

$$V_{cd} f^\pi_{+,D}(0) = 0.1374 \pm 0.0038 \pm 0.0022 \pm 0.0009 ,$$

$r_1 = -1.31 \pm 0.70 \pm 0.43$, and $r_2 = -4.2 \pm 4.0 \pm 1.9$, where the uncertainties are statistical, systematic, and the third is due to external input for the normalization. The fitted z-expansion is shown in Fig. 4. Assuming unitarity of the CKM-matrix gives $|V_{cd}| = |V_{us}| = 0.2252 \pm 0.0009$ [6], such that the fitted normalization can be used to extract $f^\pi_{+,D}(0) = 0.610 \pm 0.017 \pm 0.010 \pm 0.005$. Conversely, Lattice QCD can be used to constrain $f^\pi_{+,D}(0) = 0.666 \pm 0.029$ [8] leading to $V_{cd} = 0.206 \pm 0.007 \pm 0.009$.

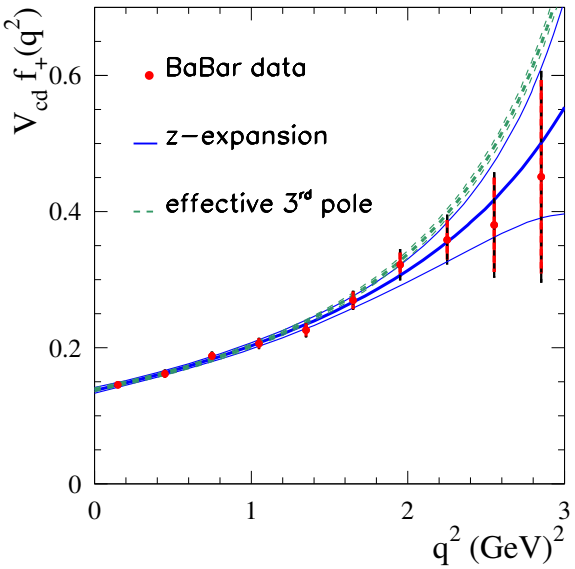

Fig. 4. Product $|V_{cd}| f^\pi_{+,D}(q^2)$ from data (red points), the z-Expansion (solid blue line), and the effective 3-pole model (dashed green line) with the corresponding uncertainty bands [1].

To gain a better understanding of the $D^0 \to \pi^- e^+ \nu$ form factor, an ansatz employing an arbitrary number of poles has been developed [9]. In this method the form factor's structure

$$f^\pi_{+,D}(q^2) = \sum_{i=0}^{\infty} \frac{Res(f^\pi_{+,D})_{D^*_i}}{m^2_{D^*_i} - q^2}$$

is exploited. The residue of each excited state is given by its mass $m_{D^*_i}$, decay constant $f_{D^*_i}$ and its coupling to the final state $D\pi$ denoted by $g_{D^*_i D\pi}$:

$$Res(f^\pi_{+,D}) = \frac{1}{2} m_{D^*_i} f_{D^*_i} g_{D^*_i D\pi}$$

The first two orders (from D^* and $D^{*\prime}$) are known from experiment [10, 11] and lattice QCD [9], thus can be used as input. In the three-pole-ansatz the next higher order is fitted to data. The result is shown in Fig. 4 and exhibits good agreement with the *BABAR* data in the low q^2 region, while it overestimates data at high q^2. In Fig. 5 it can be observed that neither the form factor based exclusively on D^* nor including D^* and $D^{*\prime}$ describes data sufficiently, hence at least a third pole is necessary to explain data. The fitted effective mass of $m_{D^{*\prime\prime}_{\text{eff}}} = (3.6 \pm 0.3)$GeV is larger than the prediction for the next pole $m_{D^{*\prime\prime}} \approx 3.1\,$GeV [12], but this is to be expected since it is an effective pole implicitly including higher orders. Moreover, this means that one additional pole at the predicted mass is not sufficient to explain data.

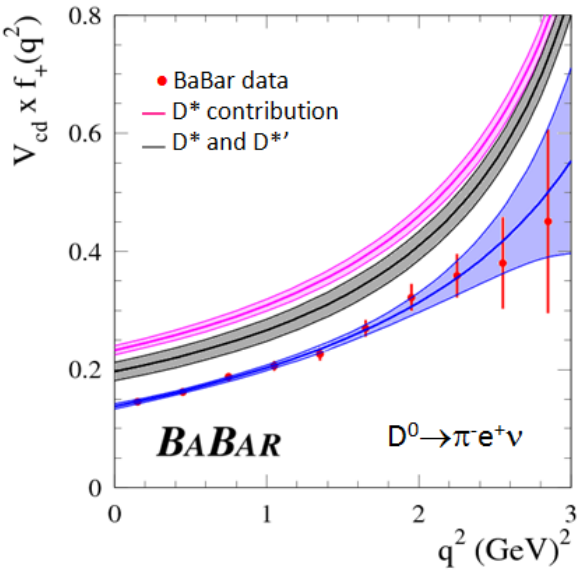

Fig. 5. Product $|V_{cd}| f^\pi_{+,D}(q^2)$ from data (red points) and the z-Expansion (solid blue line) in comparison to the effective pole model [13]. The pink curve represents the model including only the D^* contribution, while the black curve also includes the $D^{*\prime}$. The gap between data and the black line shows the necessity of at least one more pole to describe data.

5 Implications for $V_{\rm ub}$

After measuring the differential width $\mathrm{d}\Gamma(D \to \pi\ell\nu)/\mathrm{d}q^2$ and knowing that $\mathrm{d}\Gamma(B \to \pi\ell\nu)/\mathrm{d}q^2$ has already been investigated [14], the CKM matrix element $V_{\rm ub}$ can be extracted. This is achieved using the following connection between $D \to \pi\ell\nu$ and $B \to \pi\ell\nu$:

$$\left.\frac{\mathrm{d}\Gamma(B\to\pi\ell\nu)/\mathrm{d}w_B}{\mathrm{d}\Gamma(D\to\pi\ell\nu)/\mathrm{d}w_D}\right|_{w_B=w_D} = \frac{m_B}{m_D}\left|\frac{f^\pi_{+,B}}{f^\pi_{+,D}}\right|^2\left|\frac{V_{\rm ub}}{V_{\rm cd}}\right|^2 ,$$

where $w_{\rm H} = \frac{m_{\rm H}^2+m_\pi^2-q^2}{2m_{\rm H}m_\pi} = \frac{E^*_\pi}{m_\pi}$.

In this method, $\left|\frac{f^\pi_{+,B}}{f^\pi_{+,D}}\right|$ is taken as 1.8 ± 0.2, which is predicted from Lattice QCD for $w>4$, and for $V_{\rm cd}$ unitarity is assumed for the CKM matrix again. By extrapolating $\mathrm{d}\Gamma(D\to\pi\ell\nu)/\mathrm{d}w_D$ using the three poles model, $V_{\rm ub}$ is fitted to the measured $B\to\pi\ell\nu$ data. This yields

$$V_{\rm ub} = (3.65\pm0.18\pm0.40)\times10^{-3} ,$$

where the uncertainty is dominated by the form factor ratio taken from lattice calculations.

In an alternative approach, the three-pole model is fitted to the $B\to\pi\ell\nu$ data since it has been proven to work for $D\to\pi\ell\nu$. This directly gives a fitted value for $V_{\rm ub}$. For the first two poles the known masses of B^* and $B_1^{*\prime}$ [15] are used and the ratios of the residues at the different poles are constrained to be the same for D and B [16]. The third pole mass is fitted giving $m_{B^{*\prime}_{\rm eff}} = (7.4\pm0.4)$GeV, while the CKM matrix element is obtained as

$$V_{\rm ub} = (2.6\pm0.2\pm0.4)\times10^{-3} ,$$

where the uncertainty is dominated by the couplings $g_{B^{*(\prime)}B\pi}$, such that it could be improved by Lattice QCD.

6 Conclusions

The branching fraction and form factor of the channel $D^0\to\pi^-e^+\nu$ have been measured at BABAR. The implicitly included $D\to\pi$ form factor can be described by a three-pole model, also showing that two poles are not sufficient to explain the behavior observed in data. Moreover, new determinations of the CKM matrix elements $V_{\rm cd}$ and $V_{\rm ub}$ are achieved. In the case of $V_{\rm ub}$, the uncertainty could be improved significantly with new theoretical calculations, which would make it competitive with the most precise current values.

Acknowledgments

We would like to thank the organizers for this wonderful conference. We are grateful for the excellent luminosity and machine conditions provided by our PEP-II colleagues, and for the substantial dedicated effort from the computing organizations that support BABAR. *The collaborating institutions wish to thank SLAC for its support and kind hospitality. This work is supported by DOE and NSF (USA), NSERC (Canada), CEA and CNRS-IN2P3 (France), BMBF and DFG (Germany), INFN (Italy), FOM (The Netherlands), NFR (Norway), MES (Russia), MICIIN (Spain), STFC (United Kingdom). Individuals have received support from the DFG (Germany).*

References

1 J. P. Lees et al. Measurement of the $D^0\to\pi^-e^+\nu_e$ differential decay branching fraction as a function of q^2 and study of form factor parameterizations. *Phys. Rev.*, D91(5):052022, 2015.
2 Bernard Aubert et al. Measurement of the Hadronic Form Factor in $D^0\to K^-e^+\nu_e$ Decays. *Phys. Rev.*, D76:052005, 2007.
3 Geoffrey C. Fox and Stephen Wolfram. Observables for the Analysis of Event Shapes in e^+e^- Annihilation and Other Processes. *Phys. Rev. Lett.*, 41:1581, 1978.
4 Geoffrey C. Fox and Stephen Wolfram. Event Shapes in e^+e^- Annihilation. *Nucl. Phys.*, B149:413, 1979. [Erratum: Nucl. Phys.B157,543(1979)].
5 Y. Amhis et al. Averages of B-Hadron, C-Hadron, and tau-lepton properties as of early 2012. *arXiv:1207.1158*, 2012.
6 K.A. Olive et al. Review of Particle Physics. *Chin.Phys.*, C38:090001, 2014.
7 C. Glenn Boyd and Martin J. Savage. Analyticity, shapes of semileptonic form factors, and $\bar{B}\to\pi\ell\bar{\nu}$. *Phys. Rev.*, D56:303–311, 1997.
8 Sinya Aoki et al. Review of lattice results concerning low-energy particle physics. *Eur. Phys. J.*, C74:2890, 2014.
9 Damir Becirevic, Alain Le Yaouanc, Arantza Oyanguren, Patrick Roudeau, and Francesco Sanfilippo. Insight into $D/B\to\pi\ell\nu_\ell$ decay using the pole models. *arXiv:1407.1019*, 2014.
10 P. del Amo Sanchez et al. Observation of new resonances decaying to $D\pi$ and $D^*\pi$ in inclusive e^+e^- collisions near $\sqrt{s}$=10.58 GeV. *Phys. Rev.*, D82:111101, 2010.
11 J. P. Lees et al. Measurement of the $D^*(2010)^+$ natural line width and the $D^*(2010)^+ - D^0$ mass difference. *Phys. Rev.*, D88(5):052003, 2013. [Erratum: Phys. Rev.D88,no.7,079902(2013)].
12 S. Godfrey and Nathan Isgur. Mesons in a Relativized Quark Model with Chromodynamics. *Phys. Rev.*, D32:189–231, 1985.
13 Arantza Oyanguren. Measurement of the $D^0\to\pi^-e^+\nu$ branching fraction, form factor and implications for V_{ub}. In *7th International Workshop on Charm Physics (Charm 2015) Detroit, MI, USA, May 18-22, 2015*, 2015.
14 J. P. Lees et al. Branching fraction and form-factor shape measurements of exclusive charmless semileptonic B decays, and determination of $|V_{ub}|$. *Phys. Rev.*, D86:092004, 2012.
15 P. Colangelo, F. De Fazio, F. Giannuzzi, and S. Nicotri. New

meson spectroscopy with open charm and beauty. *Phys. Rev.*, D86:054024, 2012.

16 Gustavo Burdman and Joachim Kambor. Dispersive approach to semileptonic form-factors in heavy to light meson decays. *Phys. Rev.*, D55:2817–2826, 1997.